Journal of Cellular Biochemistry 101:425–441 (2007)

Site-Specific Proteolysis of Cyclooxygenase-2: A Putative Step in Inflammatory Prostaglandin E_2 Biosynthesis

Arturo Mancini,[1] Dragan V. Jovanovic,[2] Qing W. He,[2] and John A. Di Battista[2]*

[1]Department of Anatomy and Cell Biology, McGill University, Montreal (QC), Canada H3A 1A1
[2]Department of Medicine, McGill University, Montreal (QC), Canada H3A 1A1

Abstract Cyclooxygenase-2 (COX-2) catalyzes the rate-limiting step in inflammatory prostanoid biosynthesis. Transcriptional, post-transcriptional, and post-translational covalent modifications have been defined as important levels of regulation for COX-2 gene expression. Here, we describe a novel regulatory mechanism in primary human cells involving regulated, sequence-specific proteolysis of COX-2 that correlates with its catalytic activity and ultimately, the biosynthesis of prostaglandin E_2 (PGE_2). Proinflammatory cytokines induced COX-2 expression and its proteolysis into stable immunoreactive fragments of 66, 42–44, 34–36, and 28 kDa. Increased COX-2 activity (PGE_2 release) was observed coincident with the timing and degree of COX-2 proteolysis with correlation analysis confirming a linear relationship ($R^2 = 0.941$). Inhibition of induced COX-2 activity with non-steroidal anti-inflammatory drugs (NSAIDs) and COX-2 selective inhibitors also abrogated cleavage. To determine if NSAID inhibition of proteolysis was related to drug-binding-induced conformational changes in COX-2, we assayed COX-inactive NSAID derivatives that fail to bind COX-2. Interestingly, these compounds suppressed COX-2 activity and cleavage in a correlated manner, thus suggesting that the observed NSAID-induced inhibition of COX-2 cleavage occurred through COX-independent mechanisms, presumably through the inhibition of proteases involved in COX-2 processing. Corroborating this observation, COX-2 cleavage and activity were mutually suppressed by calpain/cathepsin protease inhibitors. Our data suggest that the nascent intracellular form of COX-2 may undergo limited proteolysis to attain full catalytic capacity. J. Cell. Biochem. 101: 425–441, 2007.

Key words: cyclooxygenase-2; post-translational regulation; proteolysis; proteomics; proinflammatory cytokines; primary human cells

Cyclooxygenase (COX) is the rate-limiting enzyme in the conversion of arachidonic acid to potent, multifunctional bioactive compounds called prostaglandins (PGs) [Smith et al., 2000]. COX exists as two prominent isoforms with similar structures but markedly distinct regulatory and expression profiles. COX-1 expression is constitutive, ubiquitous, and central to the production of PGs that maintain physiological homeostasis, whereas COX-2 expression is highly inducible by mitogenic and inflammatory stimuli in a variety of inflammatory and non-inflammatory cell types [Morita, 2002].

X-ray crystallographic analyses strongly suggest that both COX isoforms are homodimeric, monotopic membrane proteins targeted to the nuclear envelope and the luminal surface of the endoplasmic reticulum (ER) [Otto and Smith, 1994; Picot et al., 1994; Spencer et al., 1998]. The COX-2 monomer is organized into three distinct domains, notwithstanding the N-terminal signal peptide (amino acids (aa) 1–17) [reviewed in Kulmacz et al., 2003]: an N-terminal epidermal growth factor (EGF)-like domain (aa 18–55), an adjacent membrane-binding domain (aa 59–108) that incorporates into one leaflet of lipid membranes [Spencer et al., 1999] and a long α-helical catalytic

This article contains supplementary material, which may be viewed at the Journal of Cellular Biochemistry website at http://www.interscience.wiley.com/jpages/0730-2312/suppmat/index.html.

Grant sponsor: Canadian Institutes for Health Research; Grant number: MT11557.

*Correspondence to: John A. Di Battista, PhD, Division of Rheumatology and Clinical Immunology, Royal Victoria Hospital, McGill University Health Centre, 687 Pine Avenue W., Rm M.11.22, Montréal (QC), Canada H3A 1A1. E-mail: john.dibattista@mcgill.ca

Received 5 April 2006; Accepted 5 October 2006

DOI 10.1002/jcb.21191

domain (aa 109–572) that harbors both cyclooxygenase (cox) and peroxidase (pox) activities.

Dysregulated COX-2 expression is a common pathological denominator in various increasingly prevalent cancers, neurological and arthritic diseases [Lipsky, 1999]. As such, control mechanisms governing COX-2 gene expression have received considerable attention and studies are primarily concerned with transcriptional (including signaling cascades), post-transcriptional, and translational regulation [Tanabe and Tohnai, 2002; Espel, 2005]. It has been noted, however, that COX-2 expression (mRNA or protein) and PG biosynthesis are not always correlated, thus alluding to the possibility that COX-2 activity is regulated post-translationally. Yet, besides N-linked glycosylation [Otto and Smith, 1994] and a few reports of phosphorylation [Wun et al., 2004], little is known about this aspect of COX-2 biology and its relevance to COX-2 PG production in humans.

We, as well as other investigators, have previously reported on the kinetics and the signaling mechanisms involved in the induction of human COX-2 (hCOX-2) by proinflammatory cytokines in a number of cell phenotypes [Appleby et al., 1994; Dean et al., 1999; Faour et al., 2001, 2003]. In the present study, we re-examined this well-described phenomenon and, using more refined protein analysis, observed that activation of intracellular COX-2 enzymatic activity was correlated with limited COX-2 proteolysis. COX-2 product formation (i.e., PGE_2) followed a discrete temporal pattern and was inhibited by both COX-active and inactive non-steroidal anti-inflammatory drugs (NSAIDs) and cysteine protease inhibitors. Together, these data expose a novel association between proteolytic cleavage and catalytic activation of COX-2.

MATERIALS AND METHODS

Reagents

Recombinant human (rh) IL-1β, rhIL-17, and rhTNF-α were purchased from R&D Systems (Minneapolis, MN). Pepstatin A, leupeptin, aprotinin, *p*-amidinophenylmethylsulfonylfluoride (*p*-APMSF), (2S,3S)-*trans*-epoxysuccinyl-L-leucylamido-3-methylbutane ethyl ester (E64D), sodium fluoride (NaF), phenylmethylsulfonyl fluoride (PMSF), dithiothreitol (DTT), sodium orthovanadate, Ponceau-S, and bovine serum albumin (BSA) were products of Sigma-Aldrich Canada (Oakville, ON, Canada). COMPLETE™ protease inhibitor cocktail was obtained from Roche Diagnostics (Laval, QC, Canada). Phorbol-12-myristate-13-acetate (PMA), lipopolysaccharide (LPS), calpain inhibitor I ALLn (N-acetyl-leu-leu-Nle-ChO), γ-secreatse inhibitor XII (z-IL-CHO), N-[2-(cyclohexyloxy)-4-nitrophenyl)-methanesulfonamide] (NS-398), pyrrolidine dithiocarbamate (PDTC), prostaglandin E_2 (PGE_2), and NP-40 were purchased from Calbiochem (San Diego, CA). Sulindac sulfide and sulindac sulfone were procured from Biomol (Plymouth Meeting, PA). Indomethacin, racemic (*R*/*S*) flurbiprofen, optically pure (*R*)-flurbiprofen, and (*S*)-flurbiprofen were acquired from Cayman Chemical, Inc. (Ann Arbor, MI). Sodium dodecyl sulfate (SDS), acrylamide, bis-acrylamide, ammonium persulfate and Bio-Rad protein reagent originated from Bio-Rad Laboratories (Richmond, CA). Tris-base, EDTA, $MgCl_2$, $CaCl_2$, chloroform, dimethylsulfoxide (DMSO), anhydrous ethanol (95%), methanol (99%), trichloroacetic acid (TCA), sulfosalicylic acid, acetic acid, and formaldehyde were obtained from Fisher Scientific (Nepean, ON, Canada). Dulbecco's Modified Eagle Medium (DMEM), Trizol reagent, heat inactivated fetal bovine serum (FBS), and an antibiotic mixture [10,000 U of penicillin (base), 10,000 μg of streptomycin (base)] were products of Invitrogen-Life Technologies (Burlington, ON, Canada).

Specimen Selection and Cell Culture

Synovial lining cells (human synovial fibroblasts, HSFs) were isolated from synovial membranes (synovia) following necropsy from donors with no history of arthritic disease (mean age 30 ± 27). Additional experiments were conducted with specimens obtained from osteoarthritic (OA) and rheumatoid arthritic (RA) patients undergoing arthroplasty who were diagnosed based on the criteria developed by the American College of Rheumatology Diagnostic Subcommittee for OA/RA (mean age 67 ± 19) [Altman et al., 1986]. HSFs were released by sequential enzymatic digestion with 1 mg/ml pronase (Boehringer Mannheim Canada, Laval, QC, Canada) for 1 h, followed by 6 h with 2 mg/ml collagenase (type IA, Sigma) at 37°C in DMEM supplemented with 10% heat inactivated FBS, 100 U/ml penicillin, and 100 μg/ml streptomycin [Di Battista et al.,

1999]. Released HSFs were incubated for 1 h at 37°C in tissue culture flasks (Primaria #3824, Falcon, Lincoln Park, NJ) allowing the adherence of non-fibroblastic cells possibly present in the synovial preparation, particularly from OA and RA synovia. In addition, flow cytometric analysis (Epic II, Coulter, Miami, FL), using the anti-CD14 (fluorescein isothiocyanate, FITC) antibody, was conducted to confirm that no monocytes/macrophages were present in the synoviocyte preparation. The cells were seeded in tissue culture flasks, and cultured until confluence in DMEM supplemented with 10% FCS and antibiotics at 37°C in a humidified atmosphere of 5% CO_2/95% air. The cells were incubated in medium containing 0.5–1% FBS for 24 h before the experiments; fresh medium containing 0.5–1% FBS was added to the cells prior to the addition of drugs and/or other biological effectors. Only second or third passaged HSFs were used.

Preparation of Cell Extracts and Western Blotting

Fifty-100 μg of cellular protein extracted in RIPA buffer (50 mM Tris-HCl, pH 7.4, 150 mM NaCl, 2 mM EDTA, 1 mM PMSF, 2× COMPLETE™ protease inhibitor cocktail, 1% NP-40, 1 mM sodium orthovanadate, and 1 mM NaF), from control and treated cells, were subjected to two-dimensional gel electrophoresis (2DE) (see below) or one-dimensional SDS–PAGE (1DE) through 10–12% gels (final concentration of acrylamide) under reducing conditions. Proteins resolved by 1DE and 2DE were electrotransferred onto nitrocellulose membranes (Amersham Biosciences, Inc., Baie d'Urfé, QC, Canada). Membranes for 1DE were stained with Ponceau S solution (2% Ponceau S (w/v) in 30% trichloroacetic acid and 30% sulfosalicylic acid, diluted 1:10 in 1% (v/v) acetic acid) in order to verify transfer efficiency and normalize protein loading. Following blocking with 5% BLOTTO for 2 h at room temperature (RT) and further washing, the membranes were incubated overnight at 4°C with the primary antibody (see below) in TTBS containing 0.25% BLOTTO. The secondary horseradish peroxidase (HRP)-conjugated anti-IgG antibody (1:10,000 dilution) was then incubated with the membranes for 1 h at RT, washed extensively for 30–40 min with TTBS, and rinsed with TBS at RT. Following incubation with an ECL chemiluminescence reagent (Amersham Biosciences), membranes were prepared for autoradiography, exposed to Kodak (Rochester, NY) X-Omat film, and subjected to a digital densitometric analysis (1Dscan EX, Scanalytics, Inc., Fairfax, VA) for semi-quantitative measurements. The following primary antibodies were used: rabbit anti-pan-human COX-2 (1:7,500 dilution); rabbit anti-human mPGE Synthase-1, epitope aa 59–75 (Cayman Chemical Co.; 1:800 dilution); rabbit anti-human COX-2 (H-62), epitope aa 50–111 N-terminal (1:500 dilution), and mouse anti-human COX-2 (29), epitope aa 580–598 C-terminal (1:200 dilution) (Santa Cruz Biotechnology, Inc., Santa Cruz, CA). HRP-conjugated secondary antibodies anti-rabbit IgG (1:2,000 dilution) and anti-mouse IgG (1:2,000 dilution) were products from Cell Signaling Technology, Inc. (Beverly, MA).

Analysis of COX-2 Proteolysis by Two-Dimensional Electrophoresis

Total protein extracts (isolated as described above) from control and treated cells were prepared for 2DE using Amersham Biosciences' 2-D Clean-Up Kit exactly as per the manufacturer's instructions. Fifty-100 μg of the purified protein from each sample were resuspended in 160 μl rehydration buffer (7 M Urea, 2 M Thiourea, 4% CHAPS, 10 mM DTT, 10 mM Tris, 0.002% Bromophenol blue, and 2% ampholytes, pH 3–10 non-linear (Amersham Biosciences)) and absorbed overnight onto 7 cm pH 3–10 non-linear immobilized pH gradient (IPG) ZOOM® IEF Strips (Invitrogen) at RT. Isoelectric focusing was then performed using the ZOOM® IPGRunner™ system according to the following step-voltage protocol: (1) 200 V for 20 min; (2) 450 V for 15 min; (3) 750 V for 15 min; (4) 2,000 V for 30 min. For each step, current and voltage limits were set at 1 mA and 1 W, respectively. The strips were then equilibrated for 2nd dimension electrophoresis by separate, 15 min RT incubations in 5 ml reducing solution (10× NuPAGE® Sample Reducing Agent diluted to 1× in 1× NuPAGE® LDS Sample Buffer) and then 5 ml alkylating solution (116 mg iodoacetamide dissolved in 1× NuPAGE® LDS Sample Buffer). Subsequently, individual strips were positioned on 4–12% NUPAGE® Novex Bis-Tris gels (Invitrogen) and embedded in 0.5% agarose (wt/vol). Electrophoresis was conducted in 1× MOPS running buffer for 50 min at 200 V. The proteins on each gel were

then electrotransferred onto separate nitrocellulose membranes (Amersham Biosciences) and prepared for immunoblotting with the appropriate antibody, as described previously.

Immunoprecipitation of COX-2 Proteolytic Products and Sequencing by Mass Spectrometry

HSFs ($\sim 10^7$) incubated as indicated previously were stimulated with 5.7 pM IL-1β for a 16 h period. Subsequent to stimulation, HSFs were prepared for the immunoprecipitation of COX-2 as follows. Cells were washed thoroughly and scraped in ice-cold PBS. Cells were then pelleted and lysed in ice-cold RIPA buffer; cleared lysates were collected in a common tube and used in a large-scale COX-2 immunoprecipitation reaction. Briefly, the lysate was precleared by adding 1 μg of normal goat IgG (Santa Cruz Biotechnology) and 50 μl of a Protein G-Agarose suspension (50% v/v in PBS) per milliliter of lysate. Clearing was performed for 24 h at 4°C on a rotary shaker, followed by a 10 min, 2,500 RPM centrifugation step at 4°C. The protein content of the supernatant was quantified (Bio-Rad Dc protein assay, Bio-Rad Laboratories) and diluted to a final concentration of 1 mg/ml in RIPA buffer supplemented with 40 μl/ml of an agarose-conjugated goat anti-human COX-2 (C-20) polyclonal antibody (Santa Cruz Biotechnology). Immunoprecipitation was conducted at 4°C on a rotary shaker for 24 h, after which the immune complexes were pelleted and washed four times in cold PBS. Immunoprecipitated proteins were eluted with hot SDS sample buffer and prepared for 2DE as described in the previous section. Following the completion of the vertical electrophoresis step, the gel was fixed overnight (in 45% ddH_2O, 45% methanol, and 10% acetic acid) and transferred to the Proteomics Service Platform at the McGill University and Genome Quebec Innovation Center. The gel was silver stained as previously described [Shevchenko et al., 1996]; stained spots whose positions corresponded to those present on COX-2 immunoblots were excised and tryptic digests prepared robotically using a MassPrep Workstation (Waters Corp., Milford, MA). Twenty microliters of extracted tryptic peptides were analyzed using a 4000 Q TRAP® (MDS-Sciex, Concord, ON, Canada) liquid chromatography triple quadrupole/linear ion trap mass spectrometer. Peaklists were generated with Bioanalyst 1.4 (Mascot script) and submitted to Mascot (Matrix Science, Inc., Boston, MA) software for database search analysis against the NCBI non-redundant database. Spots identified as COX-2 were analyzed and confirmed by matrix assisted laser desorption/ionization (MALDI)-Quadrupole time-of-flight mass spectrometry (Q-Tof Ultima, Waters, Mississauga, ON, Canada) using Biolynx software included with Masslynx 4.0 (Waters).

Subcellular Fractionation

Control and treated cells were resuspended in cold homogenization buffer (0.1 M potassium phosphate buffer, pH 7.4, 1× COMPLETE™ protease inhibitor cocktail (Roche Diagnostics) and 0.25 M sucrose) and lysed by sonication on ice (4 × 5 s). Homogenates were then subjected to differential centrifugation at 1,000*g* for 10 min, 10,000*g* for 15 min, and 100,000*g* for 1 h at 4°C. The resulting nuclear (i.e., 1,000*g*), light mitochondrial-lysosomal (i.e., 10,000*g*), and microsomal (i.e., 100,000*g*) pellets were each resuspened in boiling reducing SDS sample buffer. Two milliliters of the 100,000*g* supernatant (i.e., cytosoloic/soluble fraction) were concentrated approximately 10-fold using 3K Nanosep columns (Pall Corporation, East Hills, NY) passivated with 5% Tween-20 for 2 h at RT; the concentrated samples were boiled in reducing SDS sample buffer. Fifteen micrograms of each fraction were analyzed for the presence of COX-2 fragment 3 by 1D SDS–PAGE (as previously described) using the C-terminal specific anti-human COX-2 (29) antibody (1:200 dilution) (Santa Cruz Biotechnology). Nuclear contamination of the light mitochondrial-lysosomal fractions was analyzed by reprobing the blot with the anti-Histone H2A (H-124) (1:400 dilution) (Santa Cruz Biotechnology).

Northern Blot Analysis of mRNA

Total cellular RNA was isolated (10^6 cells or 10–20 μg of RNA) using the Trizol (Invitrogen) reagent. Generally, 5 μg of total RNA were resolved on 1.2% agarose-formaldehyde gel and transferred electrophoretically (30 V overnight at 4°C) to Hybond-N™ nylon membranes (Amersham Biosciences) in 0.5× Tris/acetate/EDTA buffer, pH 7. After prehybridization for 24 h, the hybridizations were carried out at 50–55°C for 24–36 h, followed by high stringency washing at 68°C in 0.1 × SSC, 0.1% SDS. The following probes, labeled with digoxigenin-dUTP by random priming, were used for

hybridization: human COX-2 cDNA (1.8 kilobases (kb); Cayman Chemical Co.) initially cloned into the *Eco*RV site of pcDNA 1 (Invitrogen) that was released by *Pst*I and *Xho*I digestion resulting in a 1.2-kb cDNA fragment and a 780 base pair *Pst*I/*Xba*I fragment from GAPDH cDNA (1.2 kb; ATCC, Manassas, VA) that was initially cloned into a *Pst*I of pBR322 vector. This latter probe served as a control of RNA loading because GAPDH is constitutively expressed in cells used in these experiments. All of the blots were subjected to a digital densitometric analysis (1Dscan EX, Scanalytics, Inc.) for semi-quantitative measurements, and changes in COX-2 expression were always considered as a ratio, COX-2/GAPDH mRNA.

Eicosanoid Enzyme-Linked Immunosorbent Assay (ELISA)

Quantification of COX-2 activity per se would have required the measurement of its direct end-product, PGH_2. However, this is technically difficult with cells in culture due to PGH_2's instability in solution and its rapid conversion to PGE_2 by microsomal PGE synthase (mPGES)-1 (in HSFs). Given that in our cell culture system, the rate-limiting step for the production and release of PGE_2 is COX-2 activity and not the other enzymes in the PGE_2 biosynthetic cascade (i.e., cPLA2 and mPGES-1), we confidently used PGE_2 biosynthesis as a measure of COX-2 catalytic activity.

Measurements of PGE_2 in conditioned medium were performed by ELISA according to the manufacturer's instructions (R&D Systems). The intra-assay precision measured as the coefficient of variation (CV) varied from 5.8 to 17.9% while interassay precision was between 3.0 and 5.1%. The detection limit for PGE_2 in our culture medium was 13.4 pg/ml and the cross-reactivity with other typical eicosanoids was less 0.1%.

Data Quantitation

Digital densitometric analysis of Northern and Western blots was performed using 1Dscan EX (Scanalytics, Inc.). Values were normalized for differences in sample loading (as described previously) and represented graphically as a fold change relative to IL-1β-treated samples. Unless otherwise indicated, optical density (OD) and PGE_2 values used for correlation analyses were expressed relative to the corresponding value of IL-1β-treated cells (i.e., for OD values: OD of each condition/OD of IL-1β-treated cells; for PGE_2 values: PGE_2 biosynthesis (ng/10^6 cells) of each condition/PGE_2 biosynthesis of IL-1β-treated cells).

RESULTS

Time Dependent Activation of COX-2 Proteolysis and PGE_2 Release by IL-1β

The timing and degree of COX-2 proteolysis in primary human cell types known to rapidly and potently express COX-2 and its activity following proinflammatory stimulation was assessed by time-course analysis. A time-dependent increase in rh IL-1β-induced COX-2 proteolysis was observed in normal and OA primary HSFs, chondrocytes, and macrophages (data not shown). IL-1β induced rapid native HSF COX-2 protein synthesis (70–72 kDa) and proteolysis into immunoreactive fragments of 66 (F1), 42–44 (F2) and 34–36 (F3) kDa (Fig. 1A). Increased PGE_2 release (i.e., COX-2 activity) was observed in coincidence with the timing of COX-2 proteolysis (Fig. 1A). In an attempt to establish a relationship between the levels of proteolysis and COX-2 activity, we compared our initial results with the proinflammatory cytokines TNF-α and IL-17. Added at receptor saturating concentrations, the cytokines stimulated the release of PGE_2 at levels considerably lower than those observed under IL-1β stimulation. Furthermore, densitometry of the 34–36 kDa fragments (for example) from Western blots also showed notably weaker staining when compared to IL-1β-induced proteolysis (Fig. 1A, compare lane 7 to lanes 8 and 9). Since tumor-promoting phorbol esters and pathogenic cell surface determinants also regulate COX-2 [Appleby et al., 1994; Hwang, 2001], we treated HSFs with PMA (protein kinase C activator) and LPS (toll-like receptor-4 activator). As shown in Figure 1A, both effectors provoked PGE_2 release and COX-2 fragmentation although both parameters were less marked than those seen with IL-1β (Fig. 1A, compare lane 7 to lanes 10 and 11). A positive linear relationship could be established between the level of fragment production (proteolysis) under conditions described in Figure 1A and PGE_2 release (Fig. 1B). Results from a previous study have indicated that this relationship is maintained for at least 48 h following IL-1β stimulation, at which point COX-2 protein levels, fragmentation, and PGE_2 release begin to

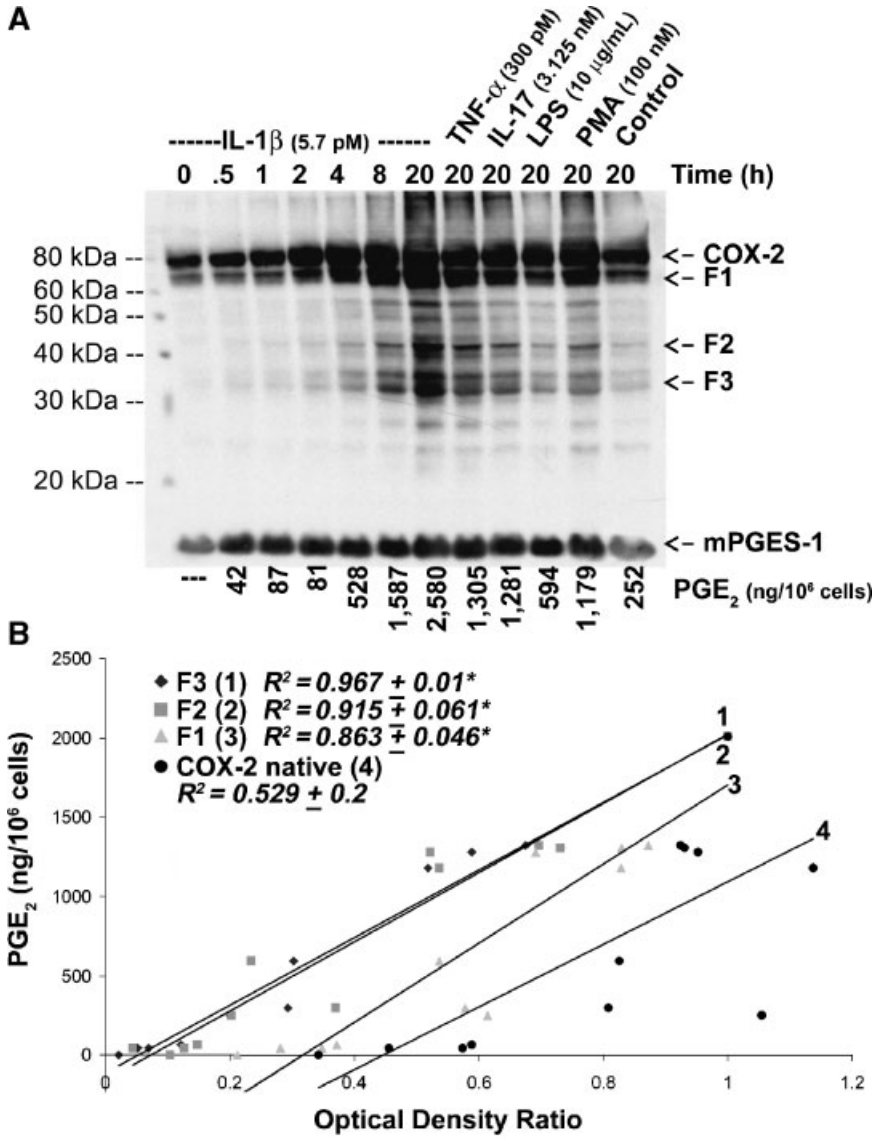

Fig. 1. Time-course of IL-1β-induced COX-2 proteolysis and prostaglandin E_2 release. Synchronized quiescent osteoarthritic human synovial fibroblasts (HSFs) were treated with IL-1β for varying times (0–20 h) or with TNF-α, IL-17, lipopolysaccharide (LPS), and phorbol myristate acetate (PMA) for 20 h. **A**: Spent culture medium was collected for ELISA analysis of prostaglandin E_2 (PGE_2); HSF protein extracts (50 μg) were used for Western blot analysis of COX-2 and microsomal PGE synthase (mPGES)-1. A representative blot and corresponding PGE_2 values (shown immediately below the blot; ng/10^6 cells) of three independent experiments is shown. **B**: Plot of the release of PGE_2 versus [optical density (OD) of fragment 1 (F1), fragment 2 (F2), fragment 3 (F3) and native (i.e., uncleaved) COX-2 for each experimental condition/OD of the respective fragment of IL-1β at 20 h] × 1. Plotted OD and PGE_2 values are expressed as a mean of three independent experiments; correlation coefficients (R^2) from the three experimental replicates were averaged using Fisher's r to z transformation and expressed as means ± SD. *, $P < 0.001$.

decline [Faour et al., 2001]. The correlation between fragment production and PGE_2 biosynthesis was of greater statistical significance (i.e., $P < 0.001$) than that between native COX-2 levels and PGE_2 production ($R^2 = 0.529$).

Quantification of PGE_2 biosynthesis in inflammatory activated HSFs almost exclusively reflects COX-2 activity. However, other enzymes in the PGE_2 biosynthetic cascade acting upstream (i.e., cytosolic phospholipase A2 (cPLA2)) or downstream (i.e., mPGES-1, in HSFs) of COX-2 can also affect PGE_2 production. To eliminate the possibility that the observed changes in PGE_2 production were a result of altered mPGES-1 expression, the Western blot in Figure 1A was reprobed for

mPGES-1. mPGES-1 protein levels were rapidly induced by IL-1β treatment (i.e., 66.4% increase relative to control within 30 min, as judged by densitometry); these levels displayed minor changes throughout the remainder of the 20 h stimulation period (±6.9%) but were not correlated to the changes in PGE_2 biosynthesis (data not shown). Identical mPGES-1 levels were evident at 20 h post-stimulation with TNF-α, IL-17, PMA, and LPS (Fig. 1A, lanes 8–12). In a previous study, HSF cPLA2 demonstrated a similar expression pattern as the one just described for mPGES-1 [Alaaeddine et al., 1999a]. Thus, the aforementioned changes in PGE_2 biosynthesis were considered strictly related to changes in COX-2 activity and collectively, the above data imply that proteolytic processing of COX-2 is directly linked to its catalytic activation.

Analysis of Proteolyic Fragments by Immunoprecipitation, Two-Dimensional Gel Electrophoresis and Peptide Sequencing by Mass Spectrometry

Cytokine-induced COX-2 proteolysis was subjected to further analysis by 2DE. To confirm the identity of the proteolytic products, we performed tandem mass spectrometric (MS/MS) sequence analysis of immunoprecipitated fragments resolved by 2DE. Silver-stained protein spots whose positions corresponded to those detected on COX-2 immunoblots were selected for analysis. As shown in Table I, five sequences were identified in the 70–72 kDa fragments (i.e., native COX-2); using an online pairwise protein sequence alignment tool [LALIGN; Huang and Miller, 1991], these sequences were localized to the membrane binding and catalytic domains of hCOX-2. Analysis of the 34–36 kDa fragments (i.e., F3) revealed two sequences; using LALIGN, both were shown to match sequences within the catalytic domain proximal to the C-terminal portion of the enzyme (Table I). The above-reported sequencing results were further confirmed by matrix-assisted laser desorption/ionization time-of-flight (MALDI-TOF) mass spectrometry.

The enhanced resolution afforded by 2DE, coupled with immunoblotting using pan and epitope-specific anti-hCOX-2 antibodies, also made it possible to identify the position of fragments within the native COX-2 holoenzyme. The anti-pan-hCOX-2 polyclonal antibody reacted specifically with the same macromolecular species detected by 1D electrophoresis (i.e., 72, 66, 54, 34–36, 28 kDa fragments) in control and IL-1β-treated cells (Fig. 2A,B). The C-terminal-specific anti-hCOX-2 (29) antibody reacted only with the holoenzyme and F3 (Fig. 2C), thus indicating that F1, F2, and the 26–28 kDa fragments lacked aa 580–598. More importantly, these data supported the notion that F1 was a genuine COX-2 cleavage product and not a hypoglycosylated form of COX-2 as reported by Otto and Smith [1994]. Given that the epitope recognized by the anti-hCOX-2 (29) antibody is located at the extreme C-terminus of the COX-2 protein, the molecular mass of the fragment recognized by this antibody (F3) is helpful in estimating the approximate cleavage site that generates this product. By this logic, we estimate that F3 may be generated by cleavage at a site within or proximal to aa 290–310 (aa 304–324 in ovine COX-1 (oCOX-1)).

Inhibition of Induced COX-2 Activity and PGE_2 Release Is Associated With Suppression of COX-2 Proteolysis

Non-selective NSAIDs and COX-2 selective inhibitors (COXIBs) are among the most widely

TABLE I. Tryptic Peptide Sequences for Fragment 3 (F3) and Native COX-2 Obtained Using Liquid Chromatography Tandem Mass Spectrometry

Amino acid sequence	Corresponding amino acid position within COX-2	Corresponding COX-2 domain
Native COX-2		
RSHLIDSPPTYNADYGY	103–119 of 604	Membrane binding/catalytic
ALPPVPDDBPTPLGVK	135–149 of 604	Catalytic
GPAFTNGLGHGVDLNHIYGETLAR	200–223 of 604	Catalytic
LKFDPELLFNKQFQYQNR	342–359 of 604	Catalytic
YQSFNEY	446–452 of 604	Catalytic
F3		
YQSFNEYR	446–453 of 604	Catalytic
SGLDDINPTVLLKE	586–598 of 604	Catalytic

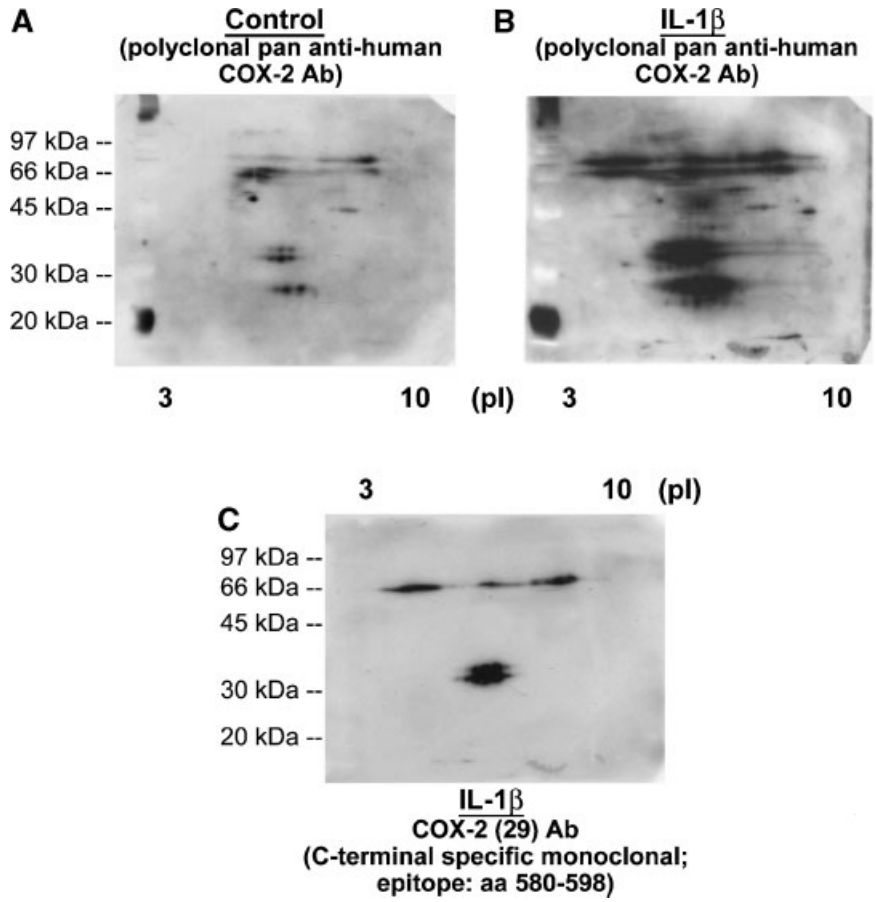

Fig. 2. Characterization of COX-2 proteolytic fragments by two-dimensional electrophoresis and Western blot analysis. Synchronized quiescent normal human synovial fibroblasts were left untreated (**A**) or stimulated with IL-1β (**B**–**C**) for 16 h. HSF total protein extracts (50 μg) were used for two-dimensional Western blot analysis of COX-2 with the indicated antibodies (Ab). Complex migratory patterns are likely due to post-translational protein modification (e.g., glycosylation, myristoylation). Abbreviations: aa, amino acids; pI, isoelectric point.

used agents in the treatment of pain and inflammation. These drugs block COX-2 catalytic activity by acting as competitive inhibitors or as radical quenchers that prevent the formation of a crucial tyrosyl radical intermediate at the cox active site. A number of NSAIDs have also been shown to target proteolytic activities both in vivo (e.g., flurbiprofen-mediated reduction of γ-secretase cleavage of amyloid precursor protein [Eriksen et al., 2003]) and in vitro [Banik et al., 2000]. In light of these findings, we examined if NSAID and COXIB-mediated inhibition of COX-2 activity in HSFs was reflected in terms of altered COX-2 proteolysis. Pharmacological doses of racemic flurbiprofen (i.e., (*R*/*S*)-flurbiprofen), indomethacin, sulindac sulfide, NS-398, and Dup-697 (not shown) decreased IL-1β-induced COX-2 proteolysis and PGE_2 biosynthesis in a highly linearly correlated fashion (i.e., OD F2 vs. PGE_2 biosynthesis: $R^2 = 0.950$, $P < 0.01$; OD F3 vs. PGE_2 biosynthesis: $R^2 = 0.985$, $P < 0.001$; Fig. 3A,B). Inhibition of PGE_2 production was not linearly correlated to drug-induced changes in COX-2 gene expression or total COX-2 protein synthesis (Figs. 3B,C and 4). Moreover, the inhibitors had no impact on mPGES-1 synthesis (Fig. 3A), suggesting that the observed decrease in PGE_2 biosynthesis strictly resulted from compromised COX-2 catalysis.

NSAID-Mediated Inhibition of COX-2 Proteolysis Occurs Through COX-Independent Mechanisms

We have previously established that COX-2 cleavage does not occur by unregulated, chemically (i.e., reactive oxygen/nitrogen species)-induced peptide bond cleavage [Miller et al., 1998]. We, therefore, reasoned that cleavage is

mediated by protease(s) and that inhibition of COX-2 proteolysis by NSAIDs can occur by two possible mechanisms: (1) drug binding to COX-2 induces changes in enzyme conformation [Kurumbail et al., 1996] that render putative cleavage sites inaccessible to protease(s) or (2) direct inhibition of the "COX-2 protease(s)." In order to distinguish between these two mechanisms, we examined the effects of optically pure (*R*)-flurbiprofen (COX inactive enantiomer of (*S*)-flurbiprofen) and sulindac sulfone (COX inactive metabolite of sulindac sulfide), both of which fail to bind COX-2 [Hawk et al., 1999]. Surprisingly, both compounds reduced HSF PGE_2 production almost as effectively as equimolar concentrations of their COX-2 active analogs (Fig. 5A). More importantly, the observed changes in PGE_2 biosynthesis corresponded directly to the changes in COX-2 proteolysis (i.e., COX-2 cleavage vs. PGE_2 biosynthesis: $R^2 = 0.835$, $P < 0.05$ for (*R*)-flurbiprofen, $R^2 = 0.927$, $P < 0.05$ for sulindac sulfone) (Fig. 5B). These results cannot be attributed to changes in IL-1β-induced COX-2 gene transcription as no significant differences (i.e., $P > 0.05$, Student's *t*-test) in COX-2 mRNA levels were evident between cells treated with IL-1β alone and those treated with IL-1β and an inactive NSAID derivative (Fig. 5C). All things considered, these data suggest that suppression of COX-2 cleavage by NSAIDs is independent of their COX-2 inhibitory activity and possibly involves the direct inhibition of one or more proteases.

Cysteine Protease Inhibitors Suppress COX-2 Proteolysis and PGE_2 Release

As a first step in the characterization of the protease(s) responsible for cleaving COX-2, we analyzed the effects of cell-permeable broad-spectrum, class-specific protease inhibitors on COX-2 proteolysis and activity. Statistically significant and linearly correlated decreases in proteolysis and activity were seen only with calpain and cathepsin inhibitors without any observable changes in mPGES-1 protein synthesis (Fig. 6A,B). Although these inhibitors demonstrated a minor but significant inhibitory activity on IL-1β-induced COX-2 gene transcription, these changes were not directly correlated to changes in either COX-2 protein expression or activity (data not shown). E64D (calpain, cathepsins B/H/L inhibitor [Tamai et al., 1986; McGowan et al., 1989]) and especially ALLn (proteasome, calpain, cathepsins B/L inhibitor [Hiwasa et al., 1990]) significantly attenuated COX-2 proteolysis (33% ± 13% and 79% ± 19% decrease, respectively) and lowered PGE_2 release by 49% ± 6% and 70% ± 18%, respectively (Fig. 6B).

In order to obtain some preliminary insight into the subcellular location of COX-2 proteolysis and thus, possibly, of the COX-2 processing enzyme(s), subcellular fractions (i.e., nuclear,

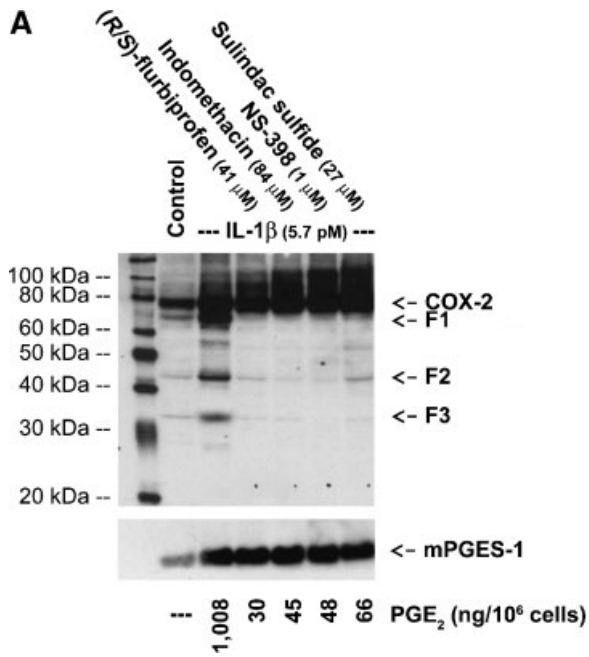

Fig. 3. Effect of non-steroidal anti-inflammatory drugs on IL-1β-induced COX-2 proteolysis and prostaglandin E_2 release. Synchronized quiescent osteoarthritic human synovial fibroblasts were pre-incubated for 1–2 h with the indicated compounds prior to treatment with IL-1β for 20 h. **A**: Total protein extracts were analyzed for COX-2 and microsomal PGE synthase (mPGES)-1 by Western blotting and conditioned medium was collected for ELISA analysis of prostaglandin E_2 (PGE_2). Control wells were incubated with vehicle in culture medium for 20 h. The figure shows a representative blot and corresponding PGE_2 values (ng/10^6 cells) of three independent experiments. **B**: Analysis of the correlation between PGE_2 biosynthesis and the parameters listed for the experimental conditions shown in (A). Values represent means from at least three independent determinations and are expressed relative those obtained for the IL-1β-treated cells. *, $P < 0.001$; #, $P < 0.01$. **C**: Analysis of the effects of the experimental conditions shown in (A) on total COX-2 protein synthesis and mRNA expression. Results are expressed as means ± S.D. ($n \geq 3$ determinations). Experimental conditions (x-axis): 1: Control; 2: IL-1β; 3: IL-1β + NS-398; 4: IL-1β + Indomethacin; 5: IL-1β + Flurbiprofen; 6: IL-1β + Sulindac sulfide. *, $P < 0.001$ versus IL-1β; #, $P < 0.01$ versus IL-1β; +, $P < 0.05$ versus IL-1β by Students *t*-test. Values for native and total COX-2 (i.e., cleaved + uncleaved) protein levels, COX-2 mRNA expression and fragments 1–3 levels were obtained by densitometry and normalized as described in the Materials and Methods section.

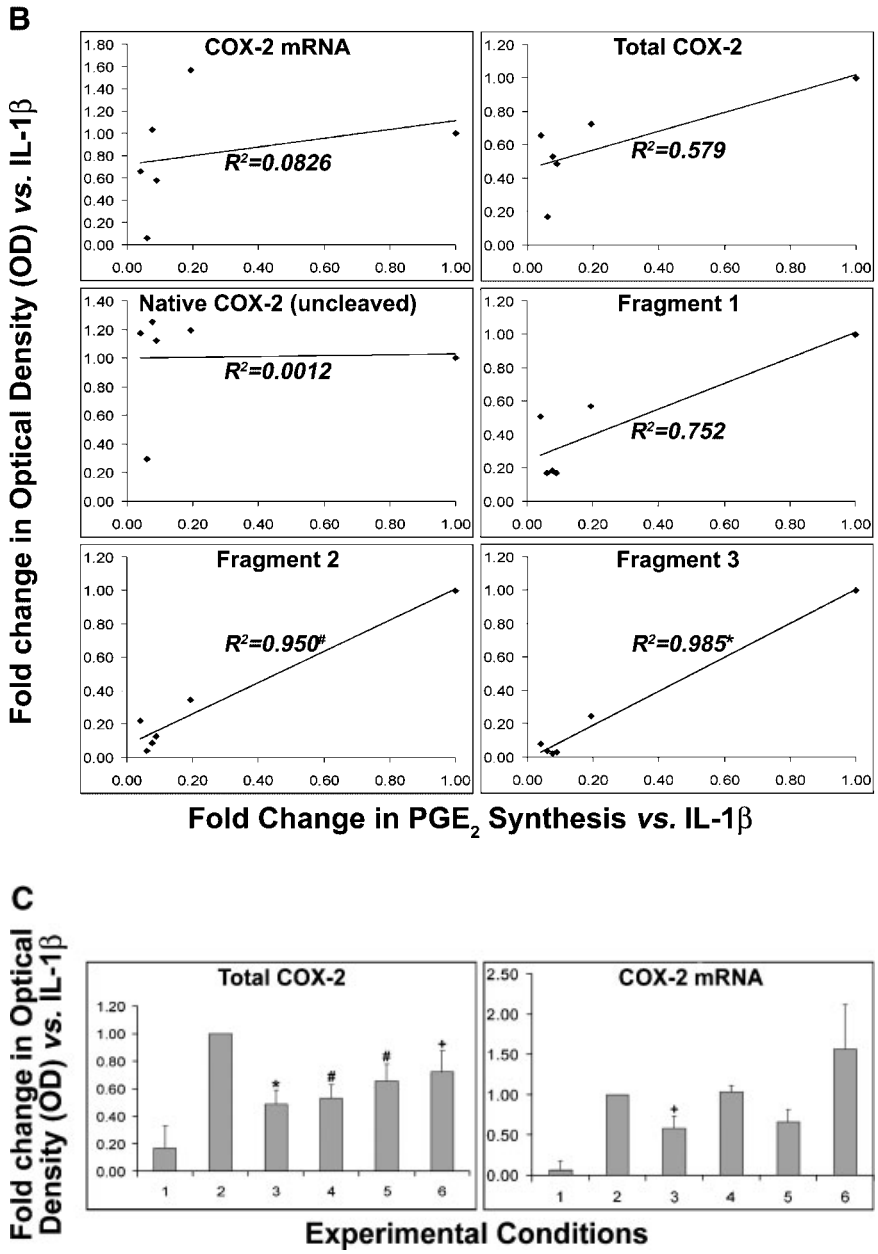

Fig. 3. (*Continued*)

cytosolic, microsomal and light mitochondrial-lysosomal) from IL-1β-treated HSFs were used for Western blot analysis of F3 (Fig. 7). COX-2 cleavage (i.e., F3) was prominent in microsomal and especially nuclear fractions, coinciding with COX-2's subcellular distribution [Spencer et al., 1998]. Interestingly, native COX-2 and the F3 cleavage product were also evident in the light mitochondrial-lysosomal fraction, corroborating protease inhibitor data suggesting the possibility of a lysosomal (i.e., cathepsin)-mediated proteolysis mechanism.

Juvenile Rheumatoid Arthritis Macrophages Exhibit Enhanced COX-2 Proteolysis and PGE_2 Biosynthesis

The pathophysiological relevance of our proteolytic activation model was revealed in primary human monocytes obtained from juvenile rheumatoid arthritic (JRA) individuals (Fig. 8). Untreated monocytes from healthy and JRA patients exhibited a cause–effect relationship between COX-2 cleavage and catalytic activity. Relative to the healthy monocytes, JRA mono-

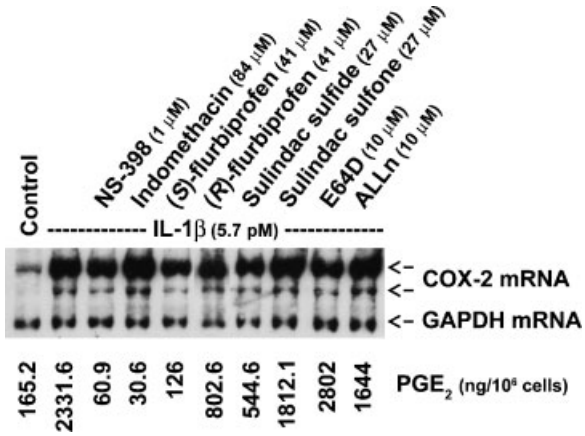

Fig. 4. Effect of protease inhibitors and COX-active and inactive non-steroidal anti-inflammatory drugs on IL-1β-induced COX-2 gene transcription. Synchronized quiescent osteoarthritic human synovial fibroblasts were pre-incubated for 1–2 h with the indicated compounds prior to treatment with IL-1β for 20 h. Monolayers were extracted for total RNA, which was prepared for Northern blot analysis of COX-2 and GAPDH mRNA. Control wells were incubated with vehicle in culture medium for 20 h. A representative blot and corresponding PGE_2 values (ng/10^6 cells) of three independent experiments is shown.

cytes displayed a 2.4-fold increase in PGE_2 biosynthesis and an additional COX-2 fragment corresponding to F3. These data thus substantiated our in vitro biochemical results linking COX-2 proteolysis to its catalytic activity.

DISCUSSION

There is now wide agreement that PGs play an indispensable role as modulators of the immune and inflammatory response and serve as key homeostatic bioregulators [Funk, 2001]. As such, much effort has been devoted to deciphering the control mechanisms governing COX-2 gene expression at transcriptional, post-transcriptional, and translational levels. Fewer reports deal with the exceedingly complex issue of COX-2 catalytic regulation and the latter concentrate on secondary and tertiary structural motifs, critical aa, and tyrosyl radical/oxidized heme intermediates as intracellular control mechanisms for cox/pox activity [Guo and Kulmacz, 2000; Rogge et al., 2004]. The results presented in this study offer a fresh view of COX-2 regulation and catalysis by demonstrating an association between induced PGE_2 biosynthesis and regulated, protease-mediated cleavage of COX-2 at a minimum of two distinct sites.

Although the mechanistic underpinnings of this system remain to be deciphered, cleavage inhibition and suppression of PGE_2 biosynthesis by class specific protease inhibitors (i.e., E64D, ALLn target calpains, and cathepsins) support a paradigm in which proteolysis results in the generation of catalytically mature COX-2. We can not discount the observation that ALLn may inhibit arachidonic acid release and PGE_2 production indirectly through blockade of NF-κB-mediated cPLA2 expression in IL-1β-stimulated HSFs [Milligan et al., 1996; Alaaeddine et al., 1999b]. However, E64D has no reported direct or indirect effects on COX-2 and cPLA2 expression or activity, thereby arguing that the decrease in PGE_2 production by protease inhibitors was probably the result of reduced COX-2 catalytic activity.

Calpain-induced COX-2 proteolysis is an appealing possibility since these calcium-activated proteases cleave substrates into discrete functional peptides and may colocalize with COX-2 by associating with ER (and Golgi) membranes on their luminal or cytosolic side [Franco and Huttenlocher, 2005]. Besides inducing COX-2, IL-1β, TNF-α, and PMA also stimulate intracellular calcium transients thus coordinating enzymic activity with substrate availability. Cathepsins, on the other hand, are mainly lysosomal proteases and their implication in COX-2 proteolysis would imply shuttling of COX-2 to lysosomes for cleavage. Interestingly, preliminary subcellular fractionation studies reveal the presence of F3 in the light mitochondrial-lysosomal fraction of HSFs (see Fig. 7) and there is a previous report on lysosome-mediated degradation of COX-2 in human umbilical vein endothelial cells [Zaric and Ruegg, 2005].

Various NSAIDs and COXIBs blocked COX-2 cleavage to varying degrees; interestingly, similar inhibitory effects were observed with COX-2-inactive NSAID derivatives incapable of binding COX-2 (i.e., sulindac sulfone, (*R*)-flurbiprofen). Metabolic conversion of inactive NSAID derivatives to their COX-2 active analogs may partly account for the observed (*R*)-flurbiprofen-induced decrease in COX-2 fragmentation and PGE_2 biosynthesis [reviewed in Wechter, 1994]; however, this phenomenon cannot explain the inhibitory effects demonstrated by sulindac sulfone since evidence of its metabolic conversion to the COX-2-active sulindac sulfide in vivo and in vitro is lacking.

Given the relatively large substrate specificity for these proteases [Storer and Ménard, 1996], it is difficult to pinpoint, at this stage of the study, the exact cleavage sites within COX-2. Nonetheless, our immunoblotting results lead us to postulate that one cleavage site lies within or proximal to aa 290–310 of the COX-2 polypeptide (aa 304–324 in oCOX-1). Based on crystallographic data, [Picot et al., 1994; Kurumbail et al., 1996], this region spans Helix 5,

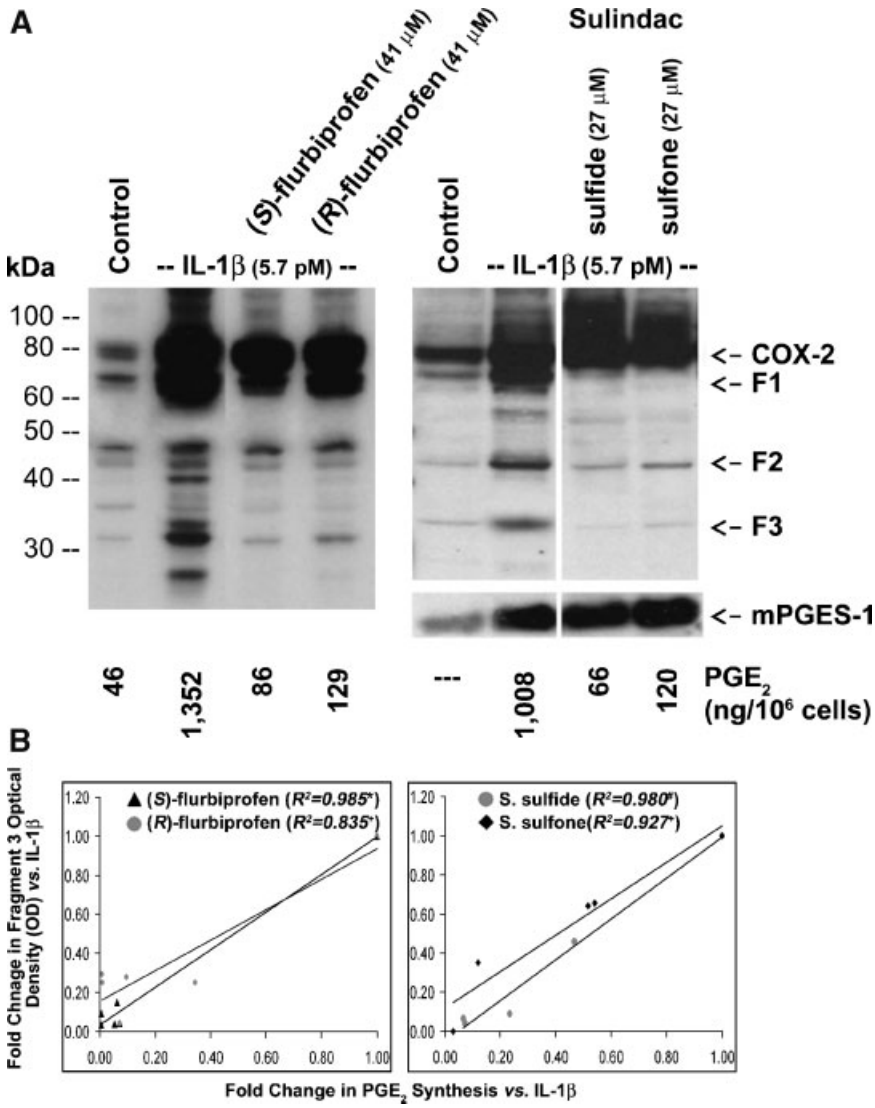

Fig. 5. Comparison of COX-active and inactive non-steroidal anti-inflammatory drug activity on IL-1β-induced COX-2 mRNA transcription, proteolysis, and prostaglandin E_2 release. Synchronized quiescent osteoarthritic human synovial fibroblasts were pre-incubated for 1–2 h with the COX-active (i.e., (*S*)-flurbiprofen and sulindac sulfide) and inactive (i.e., (*R*)-flurbiprofen and sulindac sulfone) non-steroidal anti-inflammatory drugs (NSAIDs) prior to treatment with IL-1β for 20 h. Cell monolayers were extracted for total protein and RNA. **A**: Total protein extracts were analyzed for COX-2 and microsomal PGE synthase (mPGES)-1 by Western blotting and conditioned medium was collected for ELISA analysis of prostaglandin E_2 (PGE_2). **B**: Analysis of the correlation between PGE_2 biosynthesis and COX-2 proteolysis for the experimental conditions shown in (A). Values were derived from at least three independent determinations; all values are expressed relative those obtained for the IL-1β-treated cells. Proteolysis was assessed by densitometric analysis of fragment 3 (F3). *, $P < 0.001$; #, $P < 0.01$; +, $P < 0.05$. (**C**) **Top panel**: Total RNA extracts were prepared for Northern blot analysis of COX-2 and GAPDH mRNA. A representative blot is shown. **Bottom panel**: Quantification of Northern blot results for COX-inactive NSAIDs by densitometry. Values were expressed relative those obtained for the IL-1β-treated cells and represent mean values (±SD) from at least three independent determinations. All values were normalized as described in the Materials and Methods section. All controls were incubated with vehicle in culture medium for 20 h. The blots and corresponding PGE_2 values (ng/10^6 cells) shown in this figure are each representative of three independent experiments.

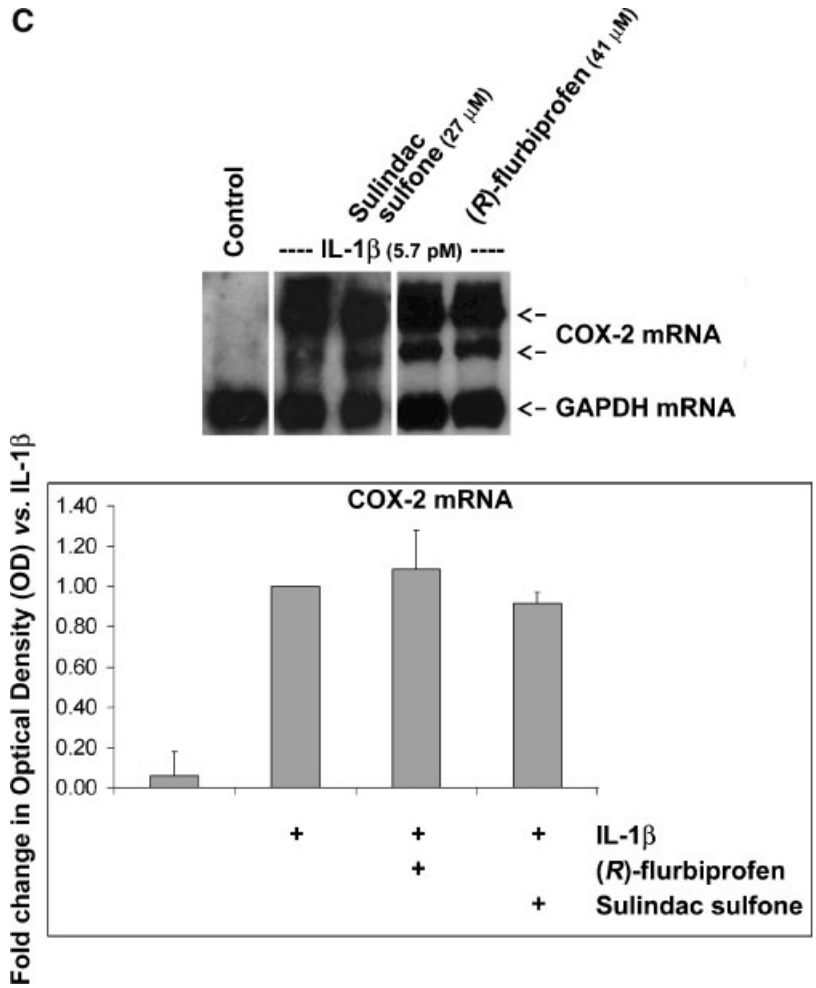

Fig. 5. (*Continued*)

which defines the floor of the cleft that includes the pox active site. The crystallographic model of COX-2 shows this helix to be located on the surface of the COX-2 monomer, diametrically opposite the membrane-binding domain and seemingly amenable to access by proteases.

The use of a primary human cell culture system was an extremely important and fundamental aspect of this study as it allowed us to analyze COX-2 in its native membrane environment. COX-2's interaction with the nuclear and ER membrane is crucial for COX-2's catalytic competence in vivo and thus, very likely an integral part of its maturation by proteolytic cleavage. Various in vitro studies using purified full-length recombinant COX-2 have demonstrated that the enzyme displays catalytic activity in the absence of cleavage [Gierse et al., 1995]. However, until COX-2 catalytic activity is assessed in situ with the enzyme in it's native environment (i.e., using cell or tissue culture), it is impossible to claim that the catalytic activity measured in vitro is in fact maximal or even comparable to that for the endogenous enzyme in an intact intracellular environment.

The majority of our experiments were conducted in HSFs since these cells are highly specialized and extremely efficient in COX-2 expression and prostanoid biosynthesis following activation with proinflammatory factors. Accordingly, HSFs provided an extremely sensitive system to study the relationship between COX-2 proteolysis and catalytic maturation in humans. Nonetheless, this relationship is not only exclusive to HSFs, but also present in various primary human cell types where COX-2 is known to play some important pathophysiological role, thereby displaying the biological importance of this mechanism. Proteolysis of transiently transfected COX-2 was also observed in various cell lines of different

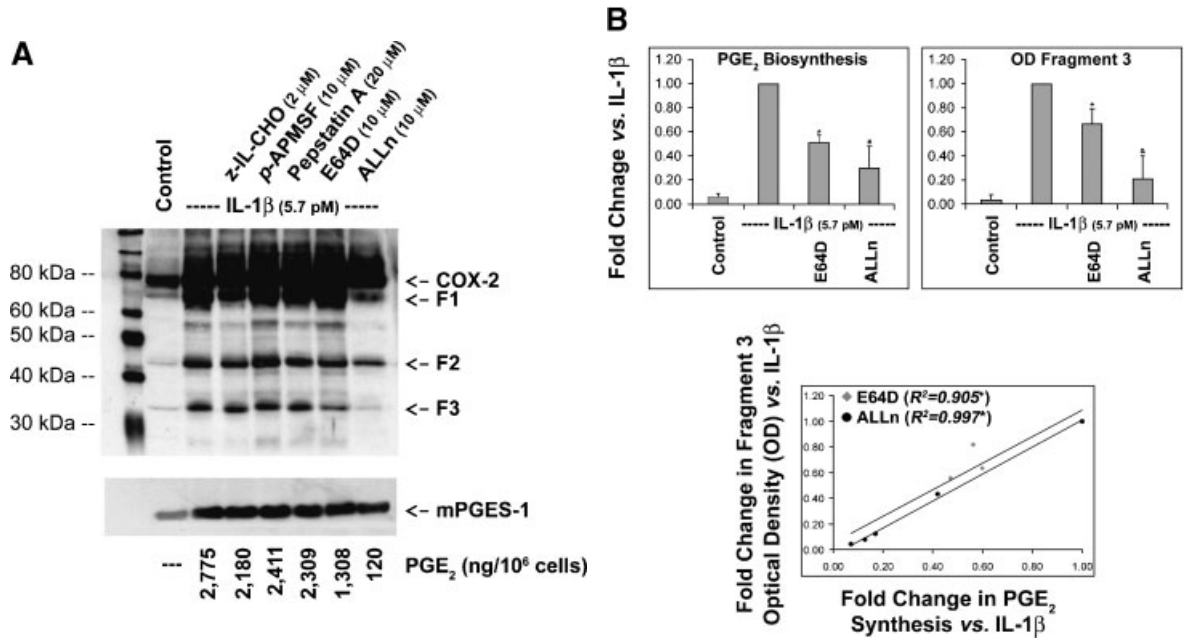

Fig. 6. Effect of protease inhibitors on IL-1β-induced COX-2 proteolysis and prostaglandin E_2 release. **A**: Synchronized quiescent osteoarthritic human synovial fibroblasts (HSFs) were pre-incubated for 1–2 h with the indicated class-specific protease inhibitors prior to treatment with IL-1β for 20 h. Total protein extracts were analyzed for COX-2 and microsomal PGE synthase (mPGES)-1 by Western blotting and conditioned medium was collected for ELISA analysis of prostaglandin E_2 (PGE_2). Control wells were incubated with vehicle in culture medium for 20 h. A representative blot and corresponding PGE_2 values (ng/10^6 cells) of three independent experiments is shown. **B**: **Top panels**: Quantification of changes in PGE_2 biosynthesis and COX-2 proteolysis (determined by densitometric analysis of fragment 3 (F3)) induced by cysteine protease inhibitors E64D and ALLn. Values were expressed relative those obtained for the IL-1β-treated cells and represent mean values ± SD from at least three independent determinations. *, $P < 0.001$ versus IL-1β; #, $P < 0.01$ versus IL-1β; &, $P < 0.02$ versus IL-1β; +, $P < 0.05$ versus IL-1β by Student's *t*-test. **Bottom panel**: Analysis of the correlation between PGE_2 biosynthesis and COX-2 fragmentation (quantified by densitometric analysis of fragment 3(F3)) for E64D and ALLn-treated HSFs. Values were derived from three independent determinations and were expressed relative those obtained for the IL-1β-treated cells. *, $P < 0.001$; +, $P < 0.05$. All values were normalized as described in the Materials and Methods section.

tissular origin (i.e., HeLa, NIH3T3, HEK293) (data not shown). However, the cleavage profile appeared to vary, albeit marginally, between the different host cell lines. These results suggest that the nature of COX-2 proteolysis may be dependent on the cell-specific expression of particular proteases.

Research on COX kinetics has clearly shown that both isoforms undergo self (i.e., "suicide")-inactivation, with catalytic activity falling to zero after about 1–2 min of catalysis (i.e., ~1,000 substrate turnovers) [reviewed in Smith et al., 2000]. This finding has led to the now widely accepted idea that proteolysis of COX-2 serves to turnover self-inactivated enzyme. Yet, the mechanistic details behind suicide-inactivation and its association to COX turnover by proteolysis have never been resolved experimentally. We propose that these two models need not necessarily be mutually exclusive and may in fact coexist in a temporal manner. The first proteolytic event would serve to generate a catalytically mature COX-2 enzyme, most likely shortly after it is synthesized; following a defined period of PGE_2 biosynthesis, the enzyme would self-inactivate and be turned over via the second proteolytic event.

Further substantiation of our model will require more direct proof of the interdependence between COX-2 proteolysis and catalytic activity. Identification of the exact cleavage site(s) by N-terminal sequencing and characterization of the "COX-2 protease(s)" by COX-2-derived peptide substrate library screening [Harris et al., 2004] will afford great assistance in obtaining such proof. These studies may lead to an understanding of the signaling mechanism by which cytokines activate proteases and whether COX-2 remains tethered to the ER membranal leaflet or is in a "soluble" phase when in its active state. In a more clinical context, our studies may not only redefine our understanding of the inflammatory process as a whole, but could also stimulate intellectual and

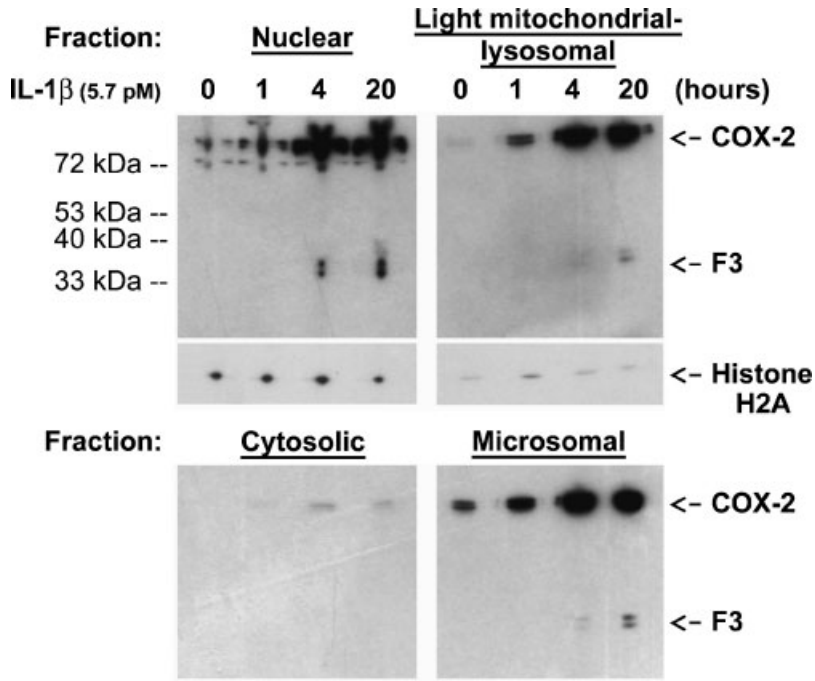

Fig. 7. Analysis of COX-2 proteolysis by subcellular fractionation. Synchronized quiescent human synovial fibroblasts (HSFs) were treated with IL-1β for the indicated times, after which they were harvested, lysed, and fractionated by differential ultracentrifugation into the fractions shown. Individual subcellular fractions were analyzed for COX-2 fragmentation using the C-terminal-specific COX-2 (29) antibody. Nuclear contamination of the light-mitochondrial-lysosomal fraction was assessed by Western blotting using an anti-histone H2A antibody.

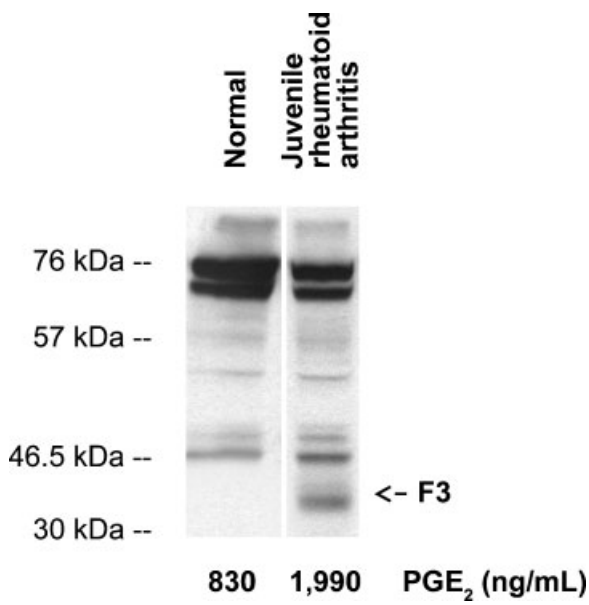

Fig. 8. COX-2 proteolysis in juvenile rheumatoid arthritis macrophages. Protein extracts from adherent, untreated normal, and arthritic peripheral monocytes were used for Western blot analysis of COX-2. Conditioned medium was collected for ELISA analysis of prostaglandin E_2 (PGE_2). Similar observations were made with other juvenile rheumatoid arthritis patient macrophage samples.

conceptual cross-fertilization into other disciplines in which proinflammatory cytokines promote pathology-inducing intracellular protein processing (Alzheimer's, multiple sclerosis, etc.).

ACKNOWLEDGMENTS

The authors thank the Canadian Institutes for Health Research and Dr. Richard R. Kulmacz for providing the pSG5-COX2 expression vector.

REFERENCES

Alaaeddine N, Di Battista JA, Pelletier JP, Kiansa K, Cloutier JM, Martel-Pelletier J. 1999a. Inhibition of tumor necrosis factor alpha-induced prostaglandin E2 production by the antiinflammatory cytokines interleukin-4, interleukin-10, and interleukin-13 in osteoarthritic synovial fibroblasts: Distinct targeting in the signaling pathways. Arthritis Rheum 42:710–718.

Alaaeddine N, Di Battista JA, Pelletier JP, Kiansa K, Cloutier JM, Martel-Pelletier J. 1999b. Differential effects of IL-8, LIF (pro-inflammatory) and IL-11 (anti-inflammatory) on TNF-alpha-induced PGE(2)release and on signalling pathways in human OA synovial fibroblasts. Cytokine 11:1020–1030.

Altman R, Asch E, Bloch D, Bole G, Borenstein D, Brandt K, Christy W, Cooke TD, Greenwald R, Hochberg M, et al. 1986. Development of criteria for the classification and reporting of osteoarthritis. Classification of osteoarthritis of the knee. Diagnostic and Therapeutic Criteria Committee of the American Rheumatism Association. Arthritis Rheum 29:1039–1049.

Appleby SB, Ristimäki A, Neilson K, Narko K, Hla T. 1994. Structure of the human cyclo-oxygenase-2 gene. Biochem J 302:723–727.

Banik NL, Matzelle D, Terry E, Gantt-Wilford G, Hogan EL. 2000. Inhibition of proteolysis by a cyclooxygenase inhibitor, indomethacin. Neurochem Res 25:1509–1515.

Dean JL, Brook M, Clark AR, Saklatvala J. 1999. p38 mitogen-activated protein kinase regulates cyclooxygenase-2 mRNA stability and transcription in lipopolysaccharide-treated human monocytes. J Biol Chem 274: 264–269.

Di Battista JA, Zhang M, Martel-Pelletier J, Fernandes J, Alaaeddine N, Pelletier JP. 1999. Enhancement of phosphorylation and transcriptional activity of the glucocorticoid receptor in human synovial fibroblasts by nimesulide, a preferential cyclooxygenase 2 inhibitor. Arthritis Rheum 42:157–166.

Eriksen JL, Sagi SA, Smith TE, Weggen S, Das P, McLendon DC, Ozols VV, Jessing KW, Zavitz KH, Koo EH, Golde TE. 2003. NSAIDs and enantiomers of flurbiprofen target gamma-secretase and lower Abeta 42 in vivo. J Clin Invest 112:440–449.

Espel E. 2005. The role of the AU-rich elements of mRNAs in controlling translation. Semin Cell Dev Biol 16:59–67.

Faour WH, He Y, He QW, de Ladurantaye M, Quintero M, Mancini A, Di Battista JA. 2001. Prostaglandin E(2) regulates the level and stability of cyclooxygenase-2 mRNA through activation of p38 mitogen-activated protein kinase in interleukin-1 beta-treated human synovial fibroblasts. J Biol Chem 276:31720–31731.

Faour WH, Mancini A, He QW, Di Battista JA. 2003. T-cell-derived interleukin-17 regulates the level and stability of cyclooxygenase-2 (COX-2) mRNA through restricted activation of the p38 mitogen-activated protein kinase cascade: Role of distal sequences in the 3′-untranslated region of COX-2 mRNA. J Biol Chem 278:26897–26907.

Franco SJ, Huttenlocher A. 2005. Regulating cell migration: Calpains make the cut. J Cell Sci 118:3829–3838.

Funk CD. 2001. Prostaglandins and leukotrienes: Advances in eicosanoid biology. Science 294:1871–1875.

Gierse JK, Hauser SD, Creely DP, Koboldt C, Rangwala SH, Isakson PC, Seibert K. 1995. Expression and selective inhibition of the constitutive and inducible forms of human cyclo-oxygenase. Biochem J 305:479–484.

Guo Q, Kulmacz RJ. 2000. Distinct influences of carboxyl terminal segment structure on function in the two isoforms of prostaglandin H synthase. Arch Biochem Biophys 384:269–279.

Harris J, Mason DE, Li J, Burdick KW, Backes BJ, Chen T, Shipway A, Van Heeke G, Gough L, Ghaemmaghami A, Shakib F, Debaene F, Winssinger N. 2004. Activity profile of dust mite allergen extract using substrate libraries and functional proteomic microarrays. Chem Biol 11:1361–1372.

Hawk E, Lubet R, Limburg P. 1999. Chemoprevention in hereditary colorectal cancer syndromes. Cancer 86: 2551–2563.

Hiwasa T, Sanada T, Sakiyama S. 1990. Cysteine proteinase inhibitors and *ras*gene products share the same biological activities including tranforming activity toward NIH3T3 mouse fibroblasts and the differentiation-inclucing activity toward PC12 rat pheochromocytoma cells. Carcinogenesis 11:75–80.

Huang X, Miller M. 1991. A time-efficient, linear-space local similarity algorithm. Adv Appl Math 12:337–357.

Hwang D. 2001. Modulation of the expression of cyclooxygenase-2 by fatty acids mediated through toll-like receptor 4-derived signaling pathways. FASEB J 15: 2556–2564.

Kulmacz RJ, van der Donk WA, Tsai AL. 2003. Comparison of the properties of prostaglandin H synthase-1 and -2. Prog Lipid Res 42:377–404.

Kurumbail RG, Stevens AM, Gierse JK, McDonald JJ, Stegeman RA, Pak JY, Gildehaus D, Miyashiro JM, Penning TD, Seibert K, Isakson PC, Stallings WC. 1996. Structural basis for selective inhibition of cyclooxygenase-2 by anti-inflammatory agents. Nature 384:644–648.

Lipsky PE. 1999. Role of cyclooxygenase-1 and -2 in health and disease. Am J Orthop 28:8–12.

McGowan EB, Becker E, Detwiler TC. 1989. Inhibition of calpain in intact platelets by the thiol protease inhibitor E-64d. Biochem Biophys Res Commun 158: 432–435.

Miller C, Zhang M, He Y, Zhao J, Pelletier JP, Martel-Pelletier J, Di Battista JA. 1998. Transcriptional induction of cyclooxygenase-2 gene by okadaic acid inhibition of phosphatase activity in human chondrocytes: Co-stimulation of AP-1 and CRE nuclear binding proteins. J Cell Biochem 69:392–413.

Milligan SA, Owens MW, Grisham MB. 1996. Inhibition of IkappaB-alpha and IkappaB-beta proteolysis by calpain inhibitor I blocks nitric oxide synthesis. Arch Biochem Biophys 335:388–395.

Morita I. 2002. Distinct functions of COX-1 and COX-2. Prostaglandins Other Lipid Mediat 68–69:165–175.

Otto JC, Smith WL. 1994. The orientation of prostaglandin endoperoxide synthases-1 and -2 in the endoplasmic reticulum. J Biol Chem 269:19868–19875.

Picot D, Loll PJ, Garavito RM. 1994. The X-ray crystal structure of the membrane protein prostaglandin H2 synthase-1. Nature 367:243–249.

Rogge CE, Liu W, Wu G, Wang LH, Kulmacz RJ, Tsai AL. 2004. Identification of Tyr504 as an alternative tyrosyl radical site in human prostaglandin H synthase-2. Biochemistry 43:1560–1568.

Shevchenko A, Wilm M, Vorm O, Mann M. 1996. Mass spectrometric sequencing of proteins silver-stained polyacrylamide gels. Anal Chem 68:850–858.

Smith WL, DeWitt DL, Garavito RM. 2000. Cyclooxygenases: Structural, cellular, and molecular biology. Annu Rev Biochem 69:145–182.

Spencer AG, Woods JW, Arakawa T, Singer II, Smith WL. 1998. Subcellular localization of prostaglandin endoperoxide H synthases-1 and -2 by immunoelectron microscopy. J Biol Chem 273:9886–9893.

Spencer AG, Thuresson E, Otto JC, Song I, Smith T, DeWitt DL, Garavito RM, Smith WL. 1999. The membrane binding domains of prostaglandin endoperoxide H synthases 1 and 2. Peptide mapping and mutational analysis. J Biol Chem 274:32936–32942.

Storer AC, Ménard R. 1996. Recent insights into cysteine protease specificity: Lessons for drug design. Perspect Drug Discovery Des 6:33–46.

Tamai M, Matsumoto K, Omura S, Koyama I, Ozawa Y, Hanada K. 1986. In vitro and in vivo inhibition of cysteine proteinases by EST, a new analog of E-64. J Pharmacobiodyn 8:672–677.

Tanabe T, Tohnai N. 2002. Cyclooxygenase isozymes and their gene structures and expression. Prostaglandins Other Lipid Mediat 68–69:95–114.

Wechter WJ. 1994. Drug chirality: On the mechanism of R-aryl propionic acid class NSAIDs. Epimerization in humans and the clinical implications for the use of racemates. J Clin Pharmacol 34:1036–1042.

Wun T, McKnight H, Tuscano JM. 2004. Increased cyclooxygenase-2 (COX-2): A potential role in the pathogenesis of lymphoma. Leuk Res 28:179–190.

Zaric J, Ruegg C. 2005. Integrin-mediated adhesion and soluble ligand binding stabilize COX-2 protein levels in endothelial cells by inducing expression and preventing degradation. J Biol Chem 280:1077–1085.